Causal information velocity in fast and slow pulse propagation in an optical ring resonator

Makoto Tomita, Hiroyuki Uesugi, Parvin Sultana, and Tohru Oishi
Department of Physics, Faculty of Science, Shizuoka University, 836, Ohya, Suruga-ku, Shizuoka 422-8529, Japan
(Received 12 August 2011; published 24 October 2011)

We examined the propagation of nonanalytical points encoded on temporally Gaussian-shaped optical pulses in fast and slow light in an optical ring resonator at $\lambda = 1.5$ μm. The temporal peak of the Gaussian pulse was either advanced or delayed, reflecting anomalous or normal dispersions in the ring resonator, relevant to under- or overcoupling conditions, respectively. The nonanalytical points were neither advanced nor delayed but appeared as they entered the ring resonator. The nonanalytical points could be interpreted as information; therefore, the experimental results suggested that information velocity is equal to the light velocity in vacuum or the background medium, independent of the group velocity. The transient behaviors at the leading and trailing edges of the nonanalytical points are discussed in terms of optical precursors.

DOI: 10.1103/PhysRevA.84.043843 PACS number(s): 42.25.Bs

I. INTRODUCTION

The speed of light is a fundamental concept in physics, and the control of light velocity is a recent interest in applications [1,2]. To date, several kinds of velocity have been discussed, including phase velocity, group velocity, energy velocity, front velocity, signal velocity, and center-of-mass velocity. Among these, group velocity v_g may be the most studied. It is now accepted that, as long as the propagation distance is short, optical pulses can travel at superluminal or even negative group velocities [3,4]. Superluminal and negative group velocities seem to contradict special relativity; hence, much effort has been made to solve this problem [5–11].

Sommerfeld and Brillouin analyzed pulse propagation using an asymptotic method and showed that the main body of the pulse follows two small precursors [5]. Most importantly, the front of the pulse always traveled at c, the velocity of light in vacuum, thereby proving that signals propagate in a relativistically causal manner. They also defined signal velocity v_s as the velocity of the main body of the pulse. As a consequence, signal velocity is $v_s \approx v_g$ when v_g is less than c and $v_s \approx c$ when v_g is larger than c. More recently, it was suggested that true information is included only in nonanalytical points encoded on the wave packets [6,7]. The arrival of the pulse peak of a smooth superluminal pulse can be predicted using Taylor expansion of the leading part of the pulse. Hence, the pulse peak has no new information in addition to that contained in the leading part of the pulse. Stenner *et al.* demonstrated that the nonanalytical points encoded in the input pulses propagate at $v_i \approx c$ through fast-gain-assisted atoms [8] and through slow light in atomic systems [9]. Specifically, they encoded ideal symbols 1 and 0 as information in an input pulse, and then the arrival of information was analyzed statistically based on the bit error rate. Causal behavior of the pulse propagation has also been demonstrated in nonlinear regimes using numerical calculations [10].

Information velocity is an important concept in physics, preserving fundamental relativistic causality, and is also important in applications, determining the ultimate bit rate in information transfer through network systems. It is therefore necessary to investigate how information velocity is determined in different systems and to clarify the underlying physics that preserves the causality. We investigated the propagation of nonanalytical points encoded on optical pulses through a ring resonator. Ring resonators are widely used in various photonic applications, including optical switches, tunable delay lines, optical buffers, nonlinear optics, and the cavity quantum electrodynamics (QED) effect [12]. Nonanalytical points can be interpreted as information. The experimental results confirmed that information velocity is equal to the velocity of light in vacuum or in the background medium, independent of the group velocity. The transient behaviors at the leading and trailing edges of the nonanalytical points are discussed in terms of optical precursors.

II. EXPERIMENTS

Figure 1 shows a schematic illustration of the experimental setup. In this study, we used a fiber ring resonator to control dispersion via the cavity loss and coupling strength between the fiber and the ring resonator. The stationary input-output characteristics can be analyzed based on the directional coupling theory [13]. The output light electric field $E_{\mathrm{out}}(\omega)$, normalized by the incident light electric field $E_{\mathrm{in}}(\omega)$, is given as

$$\frac{E_{\mathrm{out}}(\omega)}{E_{\mathrm{in}}(\omega)} = (1-\gamma)^{1/2}\left[\frac{y - x\exp(i\phi)}{1 - xy\exp(i\phi)}\right] = \sqrt{T(\omega)}\exp[i\theta(\omega)], \quad (1)$$

where $x = (1-\gamma)^{1/2}\exp(-\rho/2)$ and $y = \cos(\kappa)$ are the loss and coupling parameters, respectively, γ is the insertion loss, $\rho$is the roundtrip loss, and κ is the coupling strength. $\phi(\omega) = n\omega L_R/c$ is the phase shift in the circulation orbit, where L_R is the length of the ring resonator and n is the effective refractive index. The transmitted light intensity $T(\omega)$ as a function of ω shows a periodic dip structure due to the resonances. The dispersion relationship depends on the loss and coupling strength. For the undercoupling condition, i.e., $x < y$, the transmission phase $\theta(\omega)$ as a function of frequency shows an anomalous dispersion at the center of the resonance, and the group delay is expected to be negative, $\tau = \partial\theta/\partial\omega < 0$, corresponding to superluminal pulse propagation, namely, fast light. On the other hand, when the coupling is strong, $x > y$, the transmission phase shows

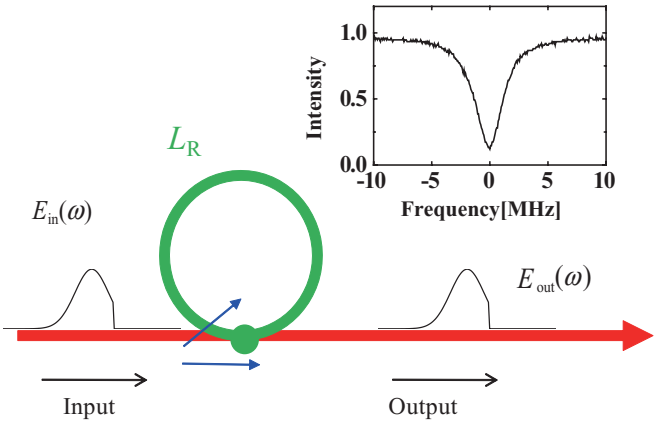

FIG. 1. (Color online) Experimental setup. The green circle represents the ring resonator. The inset shows the transmission spectrum as a function of the detuning frequency from a resonance ω_0, i.e., $\Delta\nu = (\omega - \omega_0)/2\pi$, for the undercoupling condition.

normal dispersion, and one would expect to observe slow light. In the current study, 7:93 and 20:80 couplers were used to achieve under- and overcoupling conditions, respectively. We inserted an additional loss element within the ring resonator to control the loss parameter. The physical length of the ring was $L_R = 220$ cm. An Er-fiber laser was used as the incident light source. The spectral width was 1 kHz, and the laser frequency was tuned by piezoelectric control of the cavity length. Nearly Gaussian temporal pulses were generated using a LiNbO3 (LN) modulator. The temporal duration of the pulses was $t_p = 270$ ns, the repetition rate was 100 kHz, and the incident power was 0.1 mW. The nonanalytical points were encoded on either the leading or trailing sides of Gaussian-shaped pulses. Transmission intensity through the system was observed using an InGaAs photodetector and was reordered using a 400-MHz digital oscilloscope.

The inset of Fig. 1 shows an example of transmission spectrum as a function of detuning frequency observed in continuous-wave mode, where the LN modulator was operated in open mode. The full width at half maximum (FWHM) of the resonance dips were $\delta\nu$ =3.6 and 3.7 MHz for the under- and overcoupling (not shown) conditions, respectively. Figure 2 shows the observed transmitted pulse profiles. The left and right columns correspond to the under- and overcoupling conditions, respectively. Dashed black curves are transmitted pulse profiles observed at the off-resonance laser frequency, and solid blue curves are profiles at the on-resonance frequency. The time origin was taken at the pulse-peak position observed at the off-resonance frequency. In the original Gaussian-shaped pulses, the pulse peak was advanced by $\tau = -31$ ns in Fig. 2(a) and delayed by $\tau = 84$ ns in Fig. 2(b). These experimental observations indicate that we achieved both fast and slow light in the same ring resonator system by controlling the coupling strength. The advance and delay times were calculated as $\tau = -42$ ns and $\tau = 143$ ns using Eq. (1) with the parameters $y^2 = 0.90$ ($x^2 = 0.78$) and $y^2 = 0.78$ ($x^2 = 0.93$), respectively. Slight differences between the experimental results and the calculations were attributed to the drift in the resonance frequency of the ring resonator due to the temperature change during time-resolved measurements.

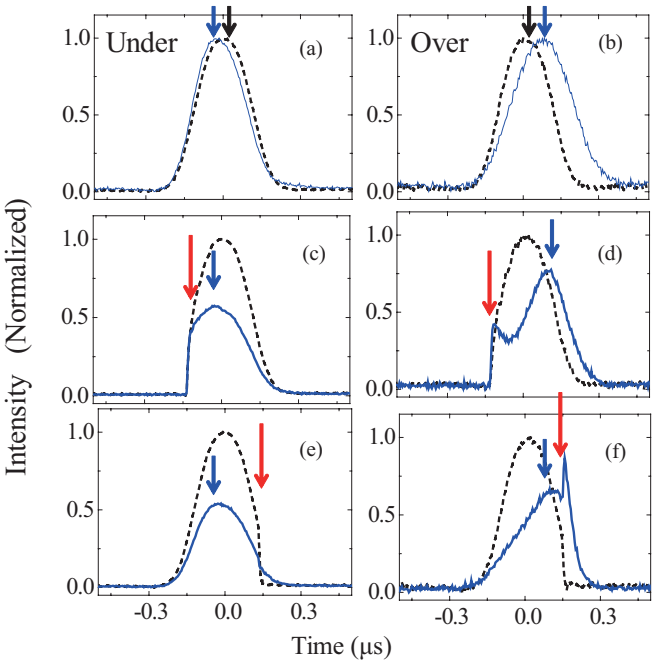

FIG. 2. (Color online) Experimental observations of the transmitted temporal pulse profiles. Dashed black curves and solid blue curves are the transmitted pulse profiles at the off- and on-resonance laser frequencies, respectively. The left and right columns correspond to the under- and overcoupling conditions, respectively. In (a) and (b), the input pulses were originally Gaussian-shaped pulses. The black and blue (gray) arrows indicate the positions of the pulse peak at the off- and on-resonance laser frequencies, respectively. In (c) and (d), the nonanalytical point was encoded on the leading side of the Gaussian pulses. In (e) and (f), the nonanalytical point was on the trailing side of the pulses. The red (light gray) arrows indicate the positions of the nonanalytical points. In (a) and (b), the profiles are normalized.

A temperature drift on the order of 10^{-3} degrees could result in a frequency shift of the resonator on the order of $\delta\nu$. This effect can shift the laser frequency into a slightly off-resonance condition, making the advancement or delay small.

Next, we investigated the propagation of nonanalytical points by encoding discontinuity at the leading and trailing sides of the pulses. Figures 2(c) and 2(d) show the pulse propagation with the nonanalytical point on the leading side. Figures 2(e) and 2(f) show similar results, but the nonanalytical point was encoded on the trailing side of the pulses. In Figs. 2(c)–2(f), the pulse peaks were still advanced or delayed depending on the coupling condition, but the nonanalytical points were neither advanced nor delayed, but rather appeared the same as they entered the ring resonator. The nonanalytical points can be interpreted as information; therefore, the experimental results agreed well with the idea that information velocity is equal to the velocity of light in vacuum or the background medium, independent of the group velocity.

Although it was confirmed that the nonanalytical points were neither advanced nor delayed, the transient behaviors in the leading and trailing edges differed depending on the coupling condition. The most prominent feature was the under- and overshooting spikes with a sharp rise followed

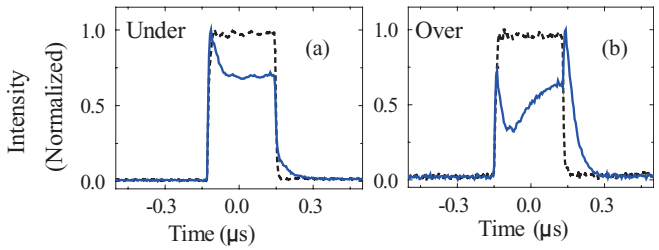

FIG. 3. (Color online) Experimental observations of the transmitted pulse profiles using square pulses for (a) the undercoupling and (b) overcoupling conditions.

by exponential decay. To observe the transient behavior more clearly, we performed similar experiments using square pulses. In this case, the square pulses had no temporal peak, but the transient structures appeared more clearly. Figure 3 shows the experimental results. In the undercoupling condition, the output intensity rose instantaneously to an initial intensity level I_R just after the input pulse was injected, and then the intensity decreased to the stationary level I_S. When the input pulse was turned off, the output intensity fell to the intensity level I_F, and then the signal decayed exponentially. In the overcoupling condition, the under- and overshooting spikes were more prominent.

The transient behaviors can be explained if we separate the total output electric field E_{tot} into the sum of the ballistic light component that bypasses the ring resonator E_{bal} and the circulated light component that passes the ring resonator E_{cir}. The circulated component passed the coupler twice; hence, the phase was shifted π rad with respect to the ballistic component. Figure 4(a) explains the transient behaviors of the undercoupling condition. When the input pulse was

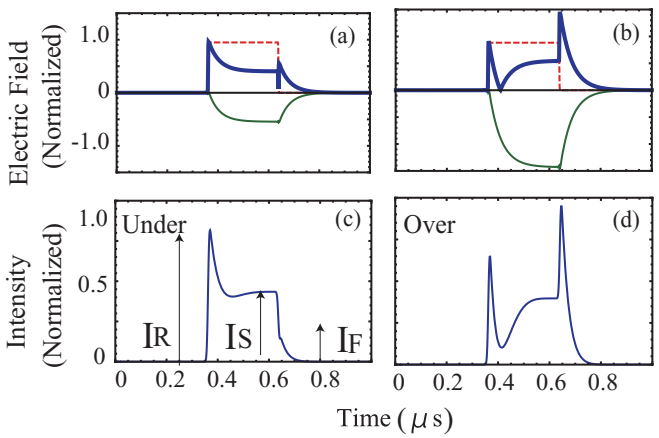

FIG. 4. (Color online) Calculated output pulses with squared input pulses. The output electric fields for (a) the undercoupling ($y^2 = 0.90$, $x^2 = 0.78$) and (b) overcoupling ($y^2 = 0.78$, $x^2 = 0.93$) conditions. Dotted red and thin solid green curves are ballistic and circulated components, respectively; the thick solid blue curves are the amplitude of the total output electric field. The circulated field (green) is plotted downward as the phase is π rad shifted. The calculated output intensity profiles for (c) the undercoupling and (d) overcoupling conditions, where the off-resonance effect was taken into account as $|\Delta\nu| < 0.8\delta\nu$. The electric field and the intensity profiles are normalized by the height of the input pulse.

turned on, the ballistic component (red dashed curve) in the transmitted light was released instantaneously at the intensity level $I_R = |E_{\text{bal}}|^2$. Then, the ring resonator began to store the light energy, with a characteristic buildup time on the order of $\tau_Q \approx 1/\delta\omega = Q/\omega$, where Q is the Q value of the cavity. The circulated component (thin green curve) gradually grew, and the transmission intensity decreased to the stationery level, $I_S = |E_{\text{bal}} - E_{\text{cir}}|^2$.Then, when the input pulse was turned off, the ballistic components disappeared instantaneously, and the intensity level fell to $I_F = |E_{\text{cir}}|^2$. Then, the light energy stored in the ring resonator escaped on a time scale of τ_Q. For the overcoupling condition [Fig. 4(b)], the circulated component (thin green curve) was stronger than the ballistic light (dashed red curve). Therefore, the total electric field became negative, $E_b - E_c$, crossing zero. This effect resulted in a deep transient dip just after the initial signal rising. To reproduce the experimentally observed intensity profiles, we considered the detuning effect that occurred due to the frequency drift during the time-resolved measurement. Figures 4(c) and 4(d) illustrate the transient output intensity profiles in which the off-resonance effect was taken into account as an integration of the signal over the condition $|\Delta\nu| < 0.8\delta\nu$. In the presence of the off-resonance effect, the circulated component had an imaginary part, and the dip was slightly smeared out. This off-resonance effect appeared stronger in the overcoupling condition because the circulated electric field was stronger in the overcoupling than the undercoupling condition.

It is noted that τ_Q also explains fast and slow light propagation for the Gaussian-shaped input pulses [Figs. 2(a) and 2(b)]. The fast and slow light in the ring resonator can be understood by an interference effect between the ballistic component and the time-delayed and phase-shifted circulated component. For the undercoupling condition, the ballistic light was stronger than the circulated light. Therefore, the trailing part of the ballistic Gaussian pulse was weakened by destructive interference with the π-rad phase-shifted and delayed circulated component. This mechanism advanced the output pulse peak with respect to the input pulse and explains the fast light. In contrast, for the overcoupling condition, the circulated light was stronger than the ballistic light, and the leading part of the circulated pulse was weakened by destructive interference with the ballistic light. This interference delayed the pulse profile with respect to the original profile and explains the slow light.

III. DISCUSSION

The sharp spikes in Fig. 4 are discussed in terms of the optical precursors. Sommerfeld and Brillouin analyzed pulse propagation using an asymptotic method and showed that the front of the pulse travels at c [5]. The pulse breaks up into two small precursors followed by a main signal. The analyses were evaluated for a broad-resonance Lorentzian medium, and it was concluded that the amplitude of the precursor was negligible. In contrast to Sommerfeld and Brillouin's analysis, it was recently suggested that the amplitude as well as the duration of the precursors can be increased by tuning the carrier frequency of the field near the narrow atomic resonances [14–19]. Optical precursors have been observed in the propagation of short pulses with steeply rising and

exponentially decaying pulses in a GaAs crystal [15]. Recently, Jeong *et al*. reported the observation of Sommerfeld and Brillouin precursors generated from a long square-modulated laser pulse propagating through cold atoms. Specifically, they evaluated the modern asymptotic theory [17] and suggested that the observed spike consisted of both Sommerfeld and Brillouin precursors [14].

In contrast to the above observations in atoms, the present system consisted of a single-stage ring resonator, corresponding to a very thin atomic sheet in which electromagnetic waves interact only once with the atom rather than propagating through an atomic gas along a distance. Asymptotic analysis is generally applicable in the case of long propagation distance limit [5]. Further, the present system is not a Lorentzian medium but produces periodic resonances. It may therefore be difficult to identify and separate Sommerfeld and Brillouin precursors and the main signal in the observations. However, the observed spikes in our experiment were similar to the resonance precursors in atomic dispersions and were based on the same underlying physics due to the following reasons. The incident laser pulse was tuned to the narrow ring-resonance mode. The spikes can be attributed to the nonresonant high- and low-frequency spectral components of the indicial pulse. The rise time was also determined by the resonance width $\delta\nu$, in good correspondence with the resonance precursors. Further, the circulated light corresponded to a secondary radiative field from the macroscopic-induced atomic polarizations.

The pulse peak was composed of Fourier components. The frequency-dependent phase shifts implemented through the resonance band moved the position of the pulse peak. As long as the propagation distance was short and most of the Fourier components were in the resonance region, the pulse peak appeared exactly at the position predicted by the group delay, even for superluminal or negative velocity. The arrival of the pulse peak, however, can be predicted based on the expansion of the previous regions of the pulse. Thus, it was thought that the arrival of pulse points that were not connected analytically to the previous regions of the pulse, i.e., nonanalytical points, could be recognized as a true signal. True information should be a signal that is intentionally sent by the sender. The rise and fall times of the discontinuous nonanalytical points in our experiments were 2.5 ns; hence, this point contained the Fourier component up to 400 MHz, which was same order as the free spectral range. The resonance width was $\delta\nu = 3.7$ MHz; hence, the discontinuous point contained high-frequency components, extending over the off-resonance region of the resonator. The photonic structure, specifically the circulated light components in this case, cannot respond to the high-frequency components, causing the precursor effect.

IV. CONCLUSION

In summary, we examined the propagation of nonanalytical points encoded on Gaussian-shaped optical pulses in fast and slow light in a ring resonator. While the peak was advanced or delayed due to under- or overcoupling, the nonanalytical points appeared as they entered the ring resonators. The nonanalytical points can be interpreted as information; therefore, the experimental results confirm that information velocity is equal to the velocity of light in vacuum or the background medium, independent of the group velocity.

[1] Nat. Photonics **2**, 447 (2008), focus issue on slow light.

[2] J. B. Khurgin and R. S. Tucker, *Slow Light: Science and Applications* (CRC Press, Boca Raton, 2008).

[3] L. J. Wang, A. Kuzmich, and A. Dogariu, Nature (London) **406**, 277 (2000).

[4] Md. Aminul Islam Talukder, Y. Amagishi, and M. Tomita, Phys. Rev. Lett. **86**, 3546 (2001).

[5] L. Brillouin, *Wave Propagation and Group Velocity* (Academic, New York, 1960).

[6] R. Y. Chiao and A. M. Steinberg, in *Progress in Optics XXXVII*, edited by E. Wolf (Elsevier, Amsterdam, 1997), p. 345.

[7] K. Wynne, Opt. Commun. **209**, 85 (2002).

[8] M. D. Stenner, D. J. Gauthier, and M. A. Neifeld, Nature (London) **425**, 695 (2003).

[9] M. D. Stenner, D. J. Gauthier, and M. A. Neifeld, Phys. Rev. Lett. **94**, 053902 (2005).

[10] G. S. Agarwal and T. N. Dey, J. Mod. Opt. **52**, 1449 (2005).

[11] G. M. Gehring, A. Schweinsberg, C. Barsi, N. Kostinski, and R. W. Boyd, Science **312**, 895 (2006).

[12] K. J. Vahala, Nature (London) **424**, 839 (2003).

[13] K. Totsuka, N. Kobayashi, and M. Tomita, Phys. Rev. Lett. **98**, 213904 (2007).

[14] K. E. Oughstun and G. C. Sherman, *Electromagnetic Pulse Propagation in Causal Dielectrics* (Springer, Berlin, 1994).

[15] J. Aaviksoo, J. Kuhl, and K. Ploog, Phys. Rev. A **44**, R5353 (1991).

[16] M. Sakai, R. Nakahara, J. Kawase, H. Kunugita, K. Ema, M. Nagai, and M. Kuwata-Gonokami, Phys. Rev. B **66**, 033302 (2002).

[17] H. Jeong, A. M. C. Dawes, and D. J. Gauthier, Phys. Rev. Lett. **96**, 143901 (2006).

[18] D. Wei, J. F. Chen, M. M. T. Loy, G. K. L. Wong, and S. Du, Phys. Rev. Lett. **103**, 093602 (2009).

[19] S. Zhang, J. F. Chen, C. Liu, M. M. T. Loy, G. K. L. Wong, and S. Du, Phys. Rev. Lett. **106**, 243602 (2011).